ORIGINAL PAPER

Evaluation of injury thresholds for predicting severe head injuries in vulnerable road users resulting from ground impact via detailed accident reconstructions

Liangliang Shi[1] · Yong Han[2,3] · Hongwu Huang[1,2,3] · Johan Davidsson[4] · Robert Thomson[4]

Abstract

The aim of this study was to evaluate the effectiveness of various head injury criteria and associated risk functions in prediction of vulnerable road users (VRUs) severe head injuries caused by ground impact during vehicle collisions. Ten VRU accidents with video information were reconstructed by using Chalmers Pedestrian Model, vehicle multi-body system models and the THUMS (Ver. 4.0.2) finite element model. The head kinematics were used to calculate injury risks for seven head kinematics-based criteria: head angular velocity and acceleration, linear acceleration, head injury criterion (HIC), head impact power (HIP) and two versions of brain injury criterion (i.e., BRIC and BrIC). In addition, the intracranial responses were used to estimate seven tissue injury criteria, Von Mises stress, shear stress, coup pressure (C.P.) and countercoup pressure (CC.P.), maximum principal strain (MPS), cumulative strain damage measure (CSDM), and dilatation damage measure (DDM). A review of the medical reports for all cases indicated that each individual suffered severe head injuries and died. The injury risks predicted through simulations were compared to the head injuries recorded in the medical or forensic reports. The results indicated that 75–100% of the reconstructed ground impact accidents injuries were correctly predicted by angular acceleration, linear acceleration, HIC, C.P., MPS and $CSDM_{0.15}$. Shear stress, CC.P. and $CSDM_{0.25}$ correctly predicted 50–75% of the reconstructed accidents injuries. For angular velocity, HIP, BRIC and BrIC, the injuries were correctly predicted for less than 50% of the reconstructed accidents. The Von Mises stress and DDM did not correctly predict any reconstructed accidents injuries. The results could help to understand the effectiveness of the brain injury criteria for future head injury evaluation.

Keywords Vulnerable road user · Severe head injury · Injury criteria · Accident reconstruction · THUMS (Ver. 4.0.2)

1 Introduction

WHO (2018) has released the Global Status Report on Road Safety, which shows that approximately 1.35 million people die each year from road traffic accidents, and more than half

✉ Yong Han
Yonghan@xmut.edu.cn

1 School of Aerospace Engineering, Xiamen University, Xiamen, China

2 School of Mechanical and Automotive Engineering, Xiamen University of Technology, Xiamen, China

3 Fujian Collaborative Innovation Center for R&D of Coach and Special Vehicle, Xiamen, China

4 Chalmers University of Technology, 412 96 Gothenburg, Sweden

of those deaths are vulnerable road users (VRUs). Studies have shown that the number of deaths and the worst injuries are mainly caused by head impacts (Mizuno and Kajzer 2000; Rosen et al. 2011). At present, car manufacturers, government agencies and researchers have made a lot of efforts to improve the protection performance of vehicles against VRUs (Young 1997; Committee 1998; Glasson et al. 2001; Shin et al. 2008; Nie and Zhou 2016; Li et al. 2017; Shi et al. 2019; Wang et al. 2019; Zou et al. 2019; Huang et al. 2020).

In order to reduce deaths of VRUs, extensive research has been carried out to identify head injury criteria and tolerance limits that can be used with crash test dummies, head impactors and human body models in the design of superior restraints and friendly vehicle front-end structures (Gadd 1966; Versace 1971; Adams et al. 1982; Gennarelli et al. 1982; Zhang et al. 2004; Kleiven 2007; Giordano and Kleiven 2014; Gabler et al. 2016). The head injury tolerance

(Gennarelli et al. 1979; Nusholtz et al. 1984; Thibault et al. 1990; Margulies and Thibault 1992; Bain and Meaney 2000) and head injury criteria (Gadd 1966; Versace 1971; Newman 1986; Hertz 1993; Newman and Shewchenko 2000; Takhounts et al. 2011; Kimpara and Iwamoto 2012; Takhounts et al. 2013) have been proposed for evaluating the human head injury risk under various crash conditions.

Currently, two types of head injury criteria have been proposed for evaluation of head injury risk. One is based on head kinematics, in which the head is considered as a single mass unit. Like the linear acceleration, it is one of the earliest fundamental parameters used to assess the risk of head injury. The European standardization commission guidelines for helmet standards stated that the maximum resultant head linear acceleration of 200–250 g could lead to the AIS 4 head injuries (Normalisation 2011). With the consideration of the time history of linear acceleration, the head injury criterion (HIC), as the only mandatory head injury criterion in automotive safety regulations, was proposed by the National Highway Traffic Safety Administration (NHTSA 1972, 1995). Although it has been used for decades as a widely accepted criterion in the vehicle safety field, some limitations of the HIC are well known. That is, only the linear loadings were considered in the equation, regardless of angular motion (Gennarelli et al. 1982; Newman 1986; Ueno and Melvin 1995). At present, the effects of angular motion on brain injury were widely investigated (Gennarelli et al. 1979, 1982; Ommaya 1985; King et al. 2003; Davidsson et al. 2009; Rowson et al. 2012). By performing a pure rotation experiment on a primate head, Margulies and Thibault (1992) proposed a diffuse axonal injuries (DAI) tolerance limit of 46.5 rad/s with an angular acceleration of 16,000 rad/s^2 for the human brain. Similarly, experiments were conducted by Davidsson et al. (2009) with the rat in the sagittal rotational plane; and from analysis of these experiments, a head injury threshold of 19 rad/s with 10,000 rad/s^2 was suggested. According to the COST 327 report (Chinn et al. 2001) and a literature review (Willinger et al. 2015), the fatal brain injury AIS 5+ could potentially occur at 10,000 rad/s^2, and a 35% risk of a brain injury of AIS 3–6 could occur at 10,000 rad/s^2. In addition to the study of injury tolerances for rotational fundamental parameters, many studies have focused on the development of rotational-based head injury criteria. For example, considering the purely rotary motion, Takhounts et al. proposed two versions of Brain Injury Criteria in 2011 and 2013, namely BRIC (Takhounts et al. 2011) and BrIC (Takhounts et al. 2013). The BRIC was developed with consideration of the maximum resultant angular velocity and acceleration, while the BrIC only considered the peak of the angular velocity around the three axes. According to the ratio of 50% head injury risk for each AIS level of HIC (NHTSA 1995),

the different injury probability curves of AIS 1–5 for the brain injury criteria were derived. In addition, Newman and Shewchenko (2000) proposed the head impact power (HIP) by considering both linear and angular accelerations along three axes of the dummy head. It was determined that a 50% risk of concussion (AIS 3) corresponded to HIP = 12.8 kW. Marjoux et al. (2008) evaluated HIP for severe head injuries based on real-world trauma cases and proposed that a 50% probability of an AIS 5 injury corresponded to 48 kW.

With the development of mathematical analysis models, the brain injury risk can be investigated based on intracranial mechanical responses which commonly are referred to injury criteria at the tissue level (Bandak and Eppinger 1994; Iwamoto et al. 2002; Takhounts et al. 2008; Wang et al. 2018). The tissue-level injury criteria are usually primarily related to the stresses (Ward et al. 1980; Anderson et al. 1999; Willinger and Baumgartner 2003; Zhang et al. 2004) and to the strains (Yoganandan et al. 2008; Gabler et al. 2016) experienced by the brain. For the stress-based criteria, Willinger and Baumgartner (2003) studied the von Mises (VM stress) and pressure through reconstruction of twenty-two American football head trauma cases and suggested that the brain VM stress was a good predictor for brain neurological lesions and that the tolerance limits to a severe brain injury with 50% risk were at 38 kPa. Zhang et al. (2004) analyzed the stress and shear stress of 24 cases of traumatic brain injury from the National Football League. She suggested that the shear stress around the brainstem could be a predictor for concussion and that a 50% probability of mild traumatic brain injury would occur at 7.8 kPa. Kang et al. (1997) reconstructed the real-world motorcycle accidents and hypothesized that a brain shear stress in the range of 11–16.5 kPa could cause severe brain injuries. As early as the 1940s, DENNY-BROWN and RUSSELL (1941) observed a positive pressure at the impact site and a negative pressure at the opposite site of the brain with animal experiments. In the study by Ward et al. (1980), the correlation between brain injury severity and the peak intracranial pressure was analyzed. The study showed that serious and fatal injuries occurred when the peak intracranial pressures exceeded 234 kPa, and the stress could be either positive or negative. In order to evaluate the brain injury which was caused by the dilatational pressure, a new computational injury metric was proposed as the dilatation damage measure (DDM) (Nusholtz et al. 1995). Takhounts et al. (2003) reanalyzed the animal experiential data (Stalnaker et al. 1978; Nusholtz et al. 1984) and found that, when DDM was equal to 7.2%, the probability of contusion occurring was 50%. This means that when 7.2% of the brain tissue volume is subjected to a negative dilatation pressure of about 100 kPa, a contusion occurs.

Another type of tissue-level criterion was based on the strain. A large number of animal studies have been performed and various thresholds of the maximal principal strain (MPS) were proposed. The MPS was considered as a predictor of concussion (Thibault et al. 1990; Shreiber et al. 1997) and of DAI (Bain and Meaney 2000). In order to investigate the cumulative volume fraction of elements with MPS exceeding a predetermined strain threshold, a new tissue-level criterion, the cumulative strain damage measurements (CSDM), was proposed (Bandak and Eppinger 1994; Takhounts et al. 2003). Moreover, various studies have been performed to evaluate this criterion with different brain finite element (FE) models (Marjoux et al. 2008; Takhounts et al. 2013; Giordano and Kleiven 2014; Sahoo et al. 2016).

For all of the aforementioned injury threshold limits and criteria, these were commonly based on experimental research with cadavers, animals and volunteers that helped to understand head injury mechanisms (Gennarelli et al. 1982; Trosseille et al. 1992; Hardy et al. 2007; Feng et al. 2010). However, due to several limitations of these experiments, e.g., having the means to carry out proper measurements, the differences in tissue properties between animals and humans, and the injury diagnostic bias of cadavers/animals, there are still many controversies in the application of the suggested tolerance limits and injury criteria in research and in the assessment of occupant restraints (Kleiven 2007). In addition, a governing belief has been that VRU head injuries are produced by the vehicle-to-VRU impact (primary impact) and that all of the above-mentioned criteria have been adopted and used in studies of the primary impact between vehicles and VRUs, or in occupant injuries studies. However, the real-world accident data analysis has indicated that the head-to-ground impacts (secondary impacts) play a very important role in the causation of head injuries (Otte and Pohlemann 2001; Badea-Romero and Lenard 2013). These studies (Ashton and Mackay 1983; Shi et al. 2018) showed that in low-velocity collisions, the head injuries caused by the ground impacts were more serious than those caused by the vehicle impacts. Since the secondary impact conditions were even more uncertain than the primary impact conditions and since there are few related studies (Shi et al. 2018, 2019), it is necessary to study the head injury tolerance limits for VRUs' head-to-ground impact.

The aim of this current study was to evaluate the effectiveness of various head injury tolerance limits and injury criteria in predicting severe head injuries caused by head-to-ground impacts. Detailed real-world VRU accidents were reconstructed using detailed injury reports and video records. Comparisons were made of the traditional accidents, and of the video films of the accident records detailed head-to-ground impact locations and scenarios were beneficial for the undertaking the accident reconstruction.

2 Method

2.1 Accident data

Ten real-world VRUs accidents were selected from the VRU-TRaffic Accident with Video database (VRU-TRAVi) (Han et al. 2018). The selection standards for VRU accidents were:

(a) Each case that was documented with detailed accident scene photos, police sketches, vehicle information, and in particular, clear surveillance videos.
(b) From the video records, the motion of the vehicle, VRU kinematic before/during/after collisions could be observed clearly.
(c) Forensic identification indicated that all VRUs died of severe head injury (AIS 4+) due to traffic accidents.

For the traveling speed, two video analysis methods were adopted to calculate the speed before the vehicle and VRU collision: One was the video frame rate method, and the other was the direct linear transformation (DLT) theory (Han et al. 2012). For the head injuries of each case, these at a minimum were assigned an abbreviated injury scale (AIS) score, while some also were assigned detailed recorded injuries such as skull fracture (SF), subdural hematoma (SDH) and subarachnoid hematoma (SAH). Table 1 summarizes the VRU categorization, vehicle types, impact velocities, VRU information and injuries, as well as the head MAIS. The data set includes three pedestrian accidents (Case C1–C3) and seven two-wheeler accidents (Case C4–C10).

2.2 Accident reconstruction

The accident reconstruction workflow is shown in Fig. 1. Firstly, the VRU's kinematics were reconstructed by using Chalmers Pedestrian Model (CPM) in the MADYMO code (Young 1997; Yang et al. 2000). The VRU's gender, stature and weight were scaled to the accident victims by scaling the standard pedestrian model of a 50th percentile male adult using the GEBOD scaling module (Cheng et al. 2002). The vehicle models were developed using ellipsoids to reproduce the detailed vehicle dimensions, and the front-end stiffnesses

Table 1 Cases reconstructed of severe head injury accidents

Case ID	VRU	Vehicle type	Impact velocity: Vehicle/VRU (km/h)	VRU information				
				Gender	Age	Stature (cm)	MAIS (head)	Head injury recorded
C1	Pedestrian (walking)	MPV	28.6/3.8	Female	79	158	5	SF, SDH, SAH
C2	Pedestrian (walking)	Sedan	28.8/1	Female	73	142	6	SDH, SAH
C3	Pedestrian (walking)	E-bicycle	31/1	Female	63	157	5	SF, SDH, SAH
C4	E-bicycle (driving)	Sedan	13.3/24.8	Male	51	166	4	SF, SDH
C5	E-bicycle (driving)	Sedan	25.2/18.6	Male	80	168	5	No record
C6	E-bicycle (driving)	Sedan	29.3/22.3	Male	56	162	5	SF, SAH
C7	E-bicycle (driving)	Sedan	29.3/22.3	Female	52	162	5	SF, SDH, SAH
C8	E-bicycle (driving)	Sedan	21/20	Female	49	150	5	SF
C9	E-bicycle (driving)	Sedan	35/20	Male	71	170	5	No record
C10	E-bicycle (driving)	SUV	49/23	Male	64	164	5	No record
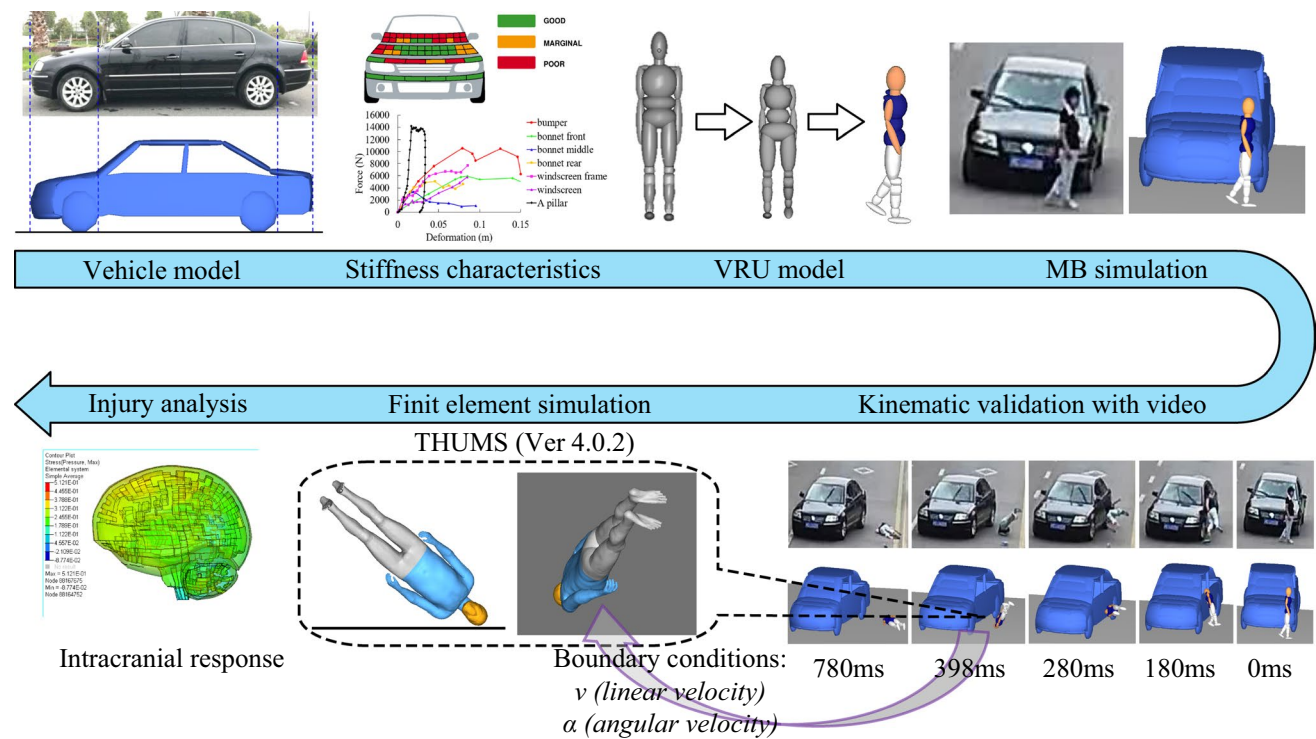
Fig. 1 The workflow implemented for the accident reconstructions and estimations of head injury criteria

were defined based on a specific vehicle's front-end stiffness determined from the Euro-NCAP test data (Martinez et al. 2007). Similarly, the stiffness characteristics of the electric bicycle were defined based on the studies of (Maki and Kajzer 2000; McLundie 2007). A total of six hinges were used to simulate the inertial motions between the bicycle components. The verifications of the reconstructions with the CPM were done by comparing the kinematics from the

simulation predictions and the results obtained from the detailed video analysis of the VRUs' kinematics and landing positions. Secondly, the head-to-ground impacts were reconstructed by using the THUMS human FE model (Ver. 4.0.2) to provide head and intracranial responses, in which the head and torso boundary conditions just prior to head-to-ground impacts were extracted from the kinematic simulation with CPM in the MADYMO code. The THUMS (Ver. 4.0.2) head
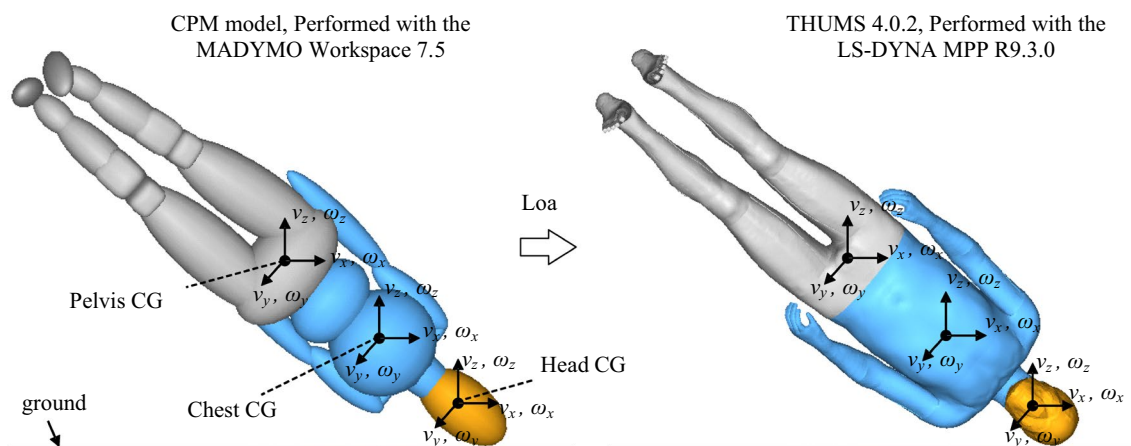
Fig. 2 The loading of boundary conditions of THUMS 4.0.2 to ground impact

model has been extensively validated (Shigeta et al. 2009; Watanabe et al. 2011). The brain motions in the head model were validated by Wang et al. (2017) using the experimental study by Hardy et al. (2001). Following our recent study (Han et al. 2019a), the head model was validated against intracranial pressure data from frontal impact experiments of human cadavers (Nahum et al. 1977). The validation results are presented in "Appendix" (Fig. 7).

Figure 2 shows the loading of the THUMS model-to-ground impact in case C2. It presents the boundary conditions at 398 ms, which was the time just before the head-to-ground impact. These boundary conditions included three-axis linear and angular velocities of the head, chest, and pelvis centers of gravity (CG) and the relative position between the pedestrian and the impacted ground location. The CPM and THUMS models were divided into three corresponding parts (head, thorax-abdomen, and lower extremity-pelvis). For each part, the three-axis linear velocities were loaded onto each component and the three-axis angular

velocities were loaded around the CG point. In all cases, the ground surface was the asphalt road and defined as a rigid body (Tamura et al. 2014, Huang et al. 2020) with a friction coefficient of 0.58 for a dry road (cases C1-C4 and C6-C10) and 0.3 for a wet road (case C5). The friction coefficient was specified to be 0.2 for the contact between the body segments and vehicle (Shi et al. 2018, 2019). The collision scenes of the real-world accidents and simulations between vehicle and VRUs in the ten cases are given in Fig. 3 and Fig. 8 of "Appendix".

2.3 Head injury criteria

Fourteen head injury criteria were calculated based on the simulation results of the accident reconstructions using the THUMS (Ver. 4.0.2) pedestrian FE model in the LS-DYNA code (Ver. MPP R9.3.0, LSTC). The head kinematics were used to calculate the head kinematics-based criteria, which were the head angular velocity (Ang. vel.), angular
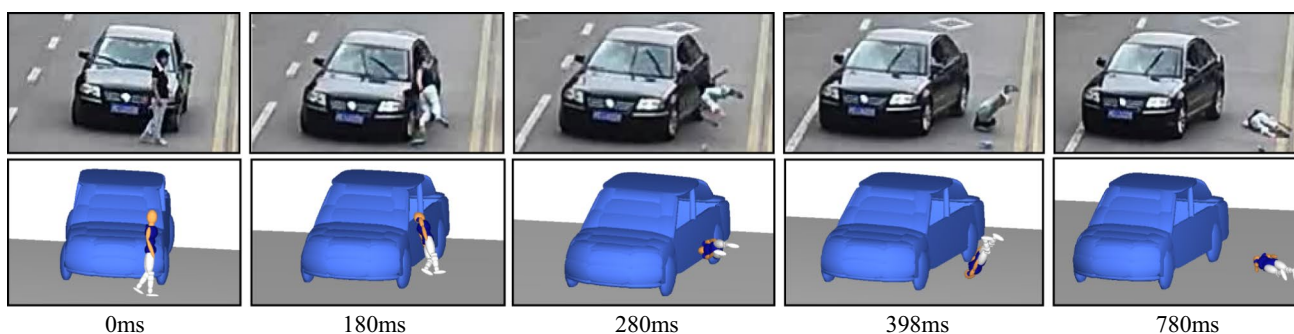
Fig. 3 The comparison between pedestrian reconstruction kinematics and video records in Case 2

Table 2 Injury threshold values used for estimations of head injury criteria

Injury criteria	50% risk of injury threshold	AIS level	References
Ang. vel	46.5 rad/s	4+	Margulies and Thibault (1992)
Ang. acc	10,000 rad/s^2	4	Chinn et al. (2001)
Lin. acc	200–250 g	4	Chinn et al. (2001), Normalisation (2011)
HIC	1440	4	Administration (1995)
HIP	48 kw	5	Marjoux et al. (2008)
BRIC	1.1	4	Takhounts et al. (2011)
BrIC	1.06	4	Takhounts et al. (2013)
VM stress	38 kPa	4+	Willinger and Baumgartner (2003)
Shear stress	11–16.5 kPa	4	Kang et al. (1997)
Coup pressure	234 kPa	5	Ward et al. (1980)
Contrecoup pressure	−234 kPa	5	Ward et al. (1980)
MPS	0.9	4	Takhounts et al. (2013)
$CSDM_{0.15}$	55%	4+	Takhounts et al. (2003)
$CSDM_{0.25}$	25%	4+	Takhounts et al. (2003)
DDM	7.2%	3	Takhounts et al. (2003)
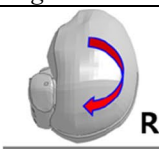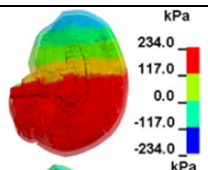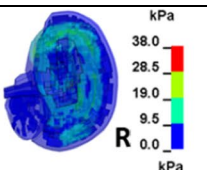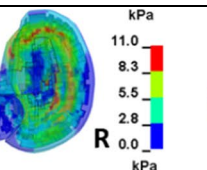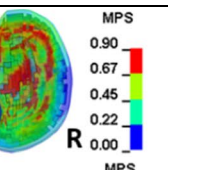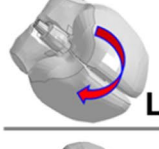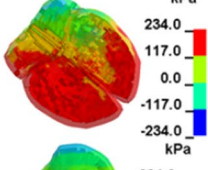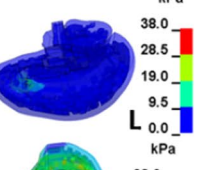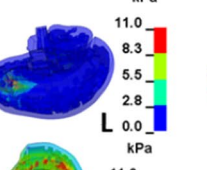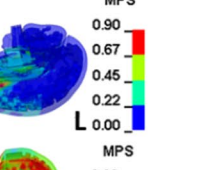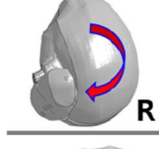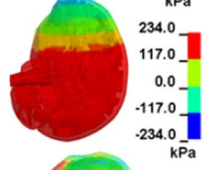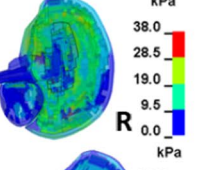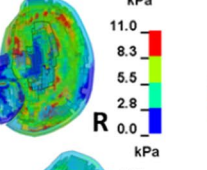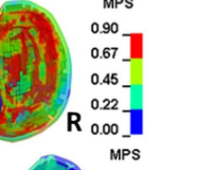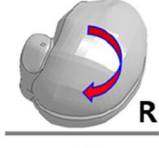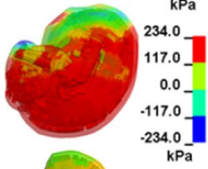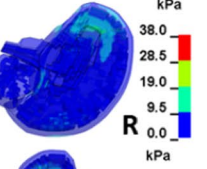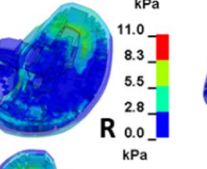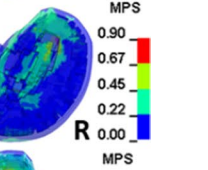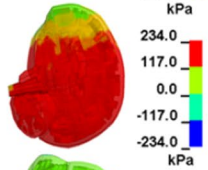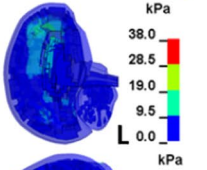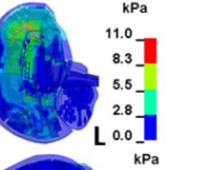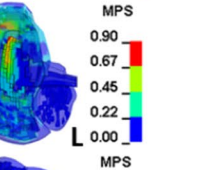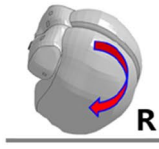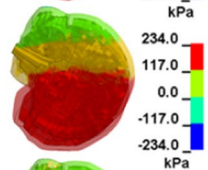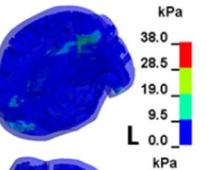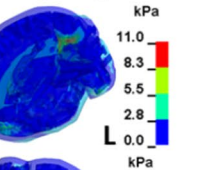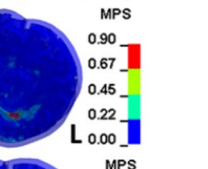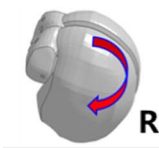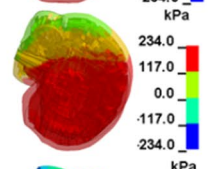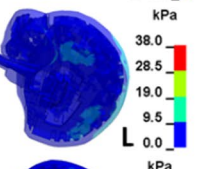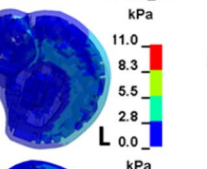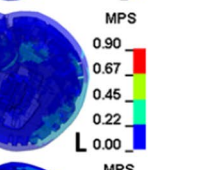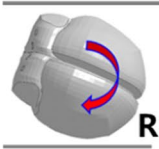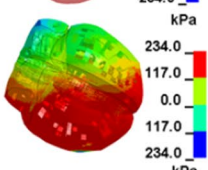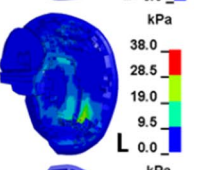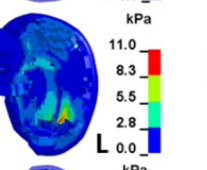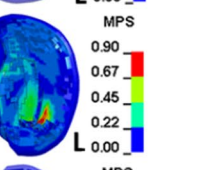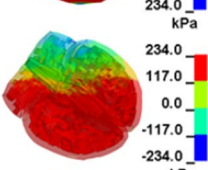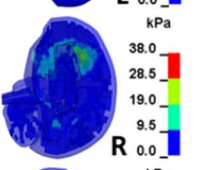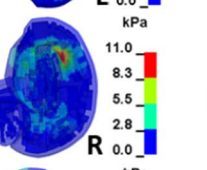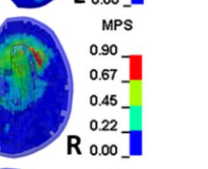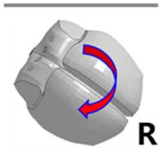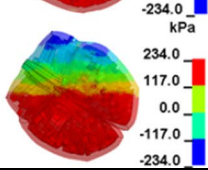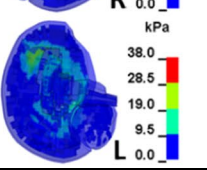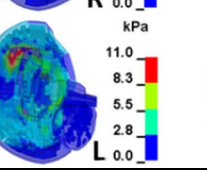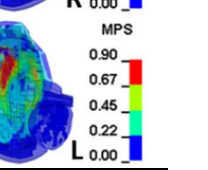
acceleration (Ang. acc.), linear acceleration (Lin. acc.), HIC, HIP, BRIC, and BrIC. In addition, the intracranial responses were used to estimate the tissue injury criteria, which included the VM stress, shear stress, coup pressure (C.P.), countercoup pressure (CC.P.), MPS, $CSDM_{0.15}$, $CSDM_{0.25}$, and DDM. Table 2 summarizes the thresholds for predicting severe head injury by the different criteria obtained through literature studies. We agree that different thresholds should be used for C.P. and CC.P. as the biomechanical (constitutive) properties of the brain tissue under tension and compression are different. However, there are few studies on cavitation responses, and it is still not clear whether cavitation occurs, or whether cavitation causes any injuries if it does occur. Research by Ward et al. (1980) states that the intracranial pressure threshold for severe and fatal injuries is approximately 34 psi (234 kPa), and these pressures can be positive or negative. This is the reference used to distinguish between C.P. and CC.P. and for using the same threshold for these two pressures. In this study, the authors focused on evaluating whether the thresholds that proposed by different studies are appropriate for the THUMS V4.0.2 head model to predict severe head injuries. The effectiveness of the criteria in predicting severe head injuries was evaluated by comparing the simulated injury criteria values to these injury thresholds.

3 Results

3.1 Kinematic response of accident reconstructions

In the ten accident cases, the VRU's head only collided with the ground and did not come into contact with the vehicle. The VRU kinematics reconstructed in the simulations were compared with the video records as shown in Fig. 3 (others are listed in Fig. 8 of "Appendix"). The reconstructed VRU kinematics showed consistent results with the video records, including the relative position between VRU and vehicle, the VRU rotation angle (Shi et al. 2018), the first VRU-to-ground contact body region, the subsequent contacts orders (Han et al. 2018), and the final position. In cases C5 and C10, the riders were found holding the handlebar tightly during the collisions, which could not be accurately reconstructed through the simulation. This caused the reconstructed kinematics of the VRUs-to-ground collisions to be slightly different than that observed from the video. However, the predicted global kinematics were still very similar to the videos. In all cases, the accident reconstruction's precision was reliable. A summary of the three-axis velocities around the head CG point at the time just before the head-to-ground impact is listed in "Appendix" Table 6.

Table 3 The maximum brain tissue criteria value for all cases

Case ID	Head-ground collison*	Pressure	VM stress	Shear stress	MPS
C1	R	kPa 234.0 / 117.0 / 0.0 / -117.0 / -234.0	kPa 38.0 / 28.5 / 19.0 / 9.5 / 0.0 R	kPa 11.0 / 8.3 / 5.5 / 2.8 / 0.0 R	MPS 0.90 / 0.67 / 0.45 / 0.22 / 0.00 R
C2	L	kPa 234.0 / 117.0 / 0.0 / -117.0 / -234.0	kPa 38.0 / 28.5 / 19.0 / 9.5 / 0.0 L	kPa 11.0 / 8.3 / 5.5 / 2.8 / 0.0 L	MPS 0.90 / 0.67 / 0.45 / 0.22 / 0.00 L
C3	R	kPa 234.0 / 117.0 / 0.0 / -117.0 / -234.0	kPa 38.0 / 28.5 / 19.0 / 9.5 / 0.0 R	kPa 11.0 / 8.3 / 5.5 / 2.8 / 0.0 R	MPS 0.90 / 0.67 / 0.45 / 0.22 / 0.00 R
C4	R	kPa 234.0 / 117.0 / 0.0 / -117.0 / -234.0	kPa 38.0 / 28.5 / 19.0 / 9.5 / 0.0 R	kPa 11.0 / 8.3 / 5.5 / 2.8 / 0.0 R	MPS 0.90 / 0.67 / 0.45 / 0.22 / 0.00 R
C5	L	kPa 234.0 / 117.0 / 0.0 / -117.0 / -234.0	kPa 38.0 / 28.5 / 19.0 / 9.5 / 0.0 L	kPa 11.0 / 8.3 / 5.5 / 2.8 / 0.0 L	MPS 0.90 / 0.67 / 0.45 / 0.22 / 0.00 L
C6	R	kPa 234.0 / 117.0 / 0.0 / -117.0 / -234.0	kPa 38.0 / 28.5 / 19.0 / 9.5 / 0.0 L	kPa 11.0 / 8.3 / 5.5 / 2.8 / 0.0 L	MPS 0.90 / 0.67 / 0.45 / 0.22 / 0.00 L
C7	R	kPa 234.0 / 117.0 / 0.0 / -117.0 / -234.0	kPa 38.0 / 28.5 / 19.0 / 9.5 / 0.0 L	kPa 11.0 / 8.3 / 5.5 / 2.8 / 0.0 L	MPS 0.90 / 0.67 / 0.45 / 0.22 / 0.00 L
C8	R	kPa 234.0 / 117.0 / 0.0 / 117.0 / 234.0	kPa 38.0 / 28.5 / 19.0 / 9.5 / 0.0 L	kPa 11.0 / 8.3 / 5.5 / 2.8 / 0.0 L	MPS 0.90 / 0.67 / 0.45 / 0.22 / 0.00 L
C9	L	kPa 234.0 / 117.0 / 0.0 / -117.0 / -234.0	kPa 38.0 / 28.5 / 19.0 / 9.5 / 0.0 R	kPa 11.0 / 8.3 / 5.5 / 2.8 / 0.0 R	MPS 0.90 / 0.67 / 0.45 / 0.22 / 0.00 R
C10	R	kPa 234.0 / 117.0 / 0.0 / -117.0 / -234.0	kPa 38.0 / 28.5 / 19.0 / 9.5 / 0.0 L	kPa 11.0 / 8.3 / 5.5 / 2.8 / 0.0 L	MPS 0.90 / 0.67 / 0.45 / 0.22 / 0.00 L

R means the right brain, L means the left brain

Table 4 The location of the maximal tissue criteria value

Case ID	Head impact side*	Maximum value region*				
		Coup pressure	Contrecoup pressure	VM stress	Shear stress	MPS
C1	R	Cerebrum_Gray_R	Stem_White_L	Cerebrum_White_R	Cerebrum_White_R	Cerebrum_Gray_R
C2	L	Cerebrum_Gray_L	Cerebellum_Gray_R	Cerebrum_Gray_L	Cerebrum_Gray_L	Cerebrum_Gray_L
C3	R	Cerebrum_Gray_L	Stem_White_L	Cerebrum_White_R	Cerebrum_White_R	Cerebrum_White_R
C4	R	Cerebrum_Gray_R	Cerebrum_Gray_R	Cerebrum_White_R	Cerebrum_White_R	Cerebrum_White_R
C5	L	Cerebrum_Gray_L	Cerebellum_Gray_R	Cerebrum_White_L	Cerebrum_White_L	Cerebrum_White_L
C6	R	Stem_Gray_R	Cerebellum_Gray_L	Cerebrum_White_L	Cerebrum_White_L	Cerebrum_Gray_L
C7	R	Cerebrum_Gray_R	Cerebellum_Gray_L	Cerebrum_White_L	Cerebrum_White_L	Cerebrum_White_L
C8	R	Cerebrum_Gray_R	Cerebellum_Gray_L	Cerebrum_White_L	Cerebrum_White_L	Cerebrum_White_L
C9	L	Cerebrum_Gray_L	Cerebrum_Gray_L	Cerebrum_Gray_R	Cerebrum_Gray_R	Cerebrum_Gray_R
C10	R	Stem_White_R	Cerebellum_Gray_L	Cerebrum_Gray_L	Cerebrum_Gray_L	Cerebrum_Gray_L

*Gray, Gray matter; White, White matter. R means the right brain, L means the left brain
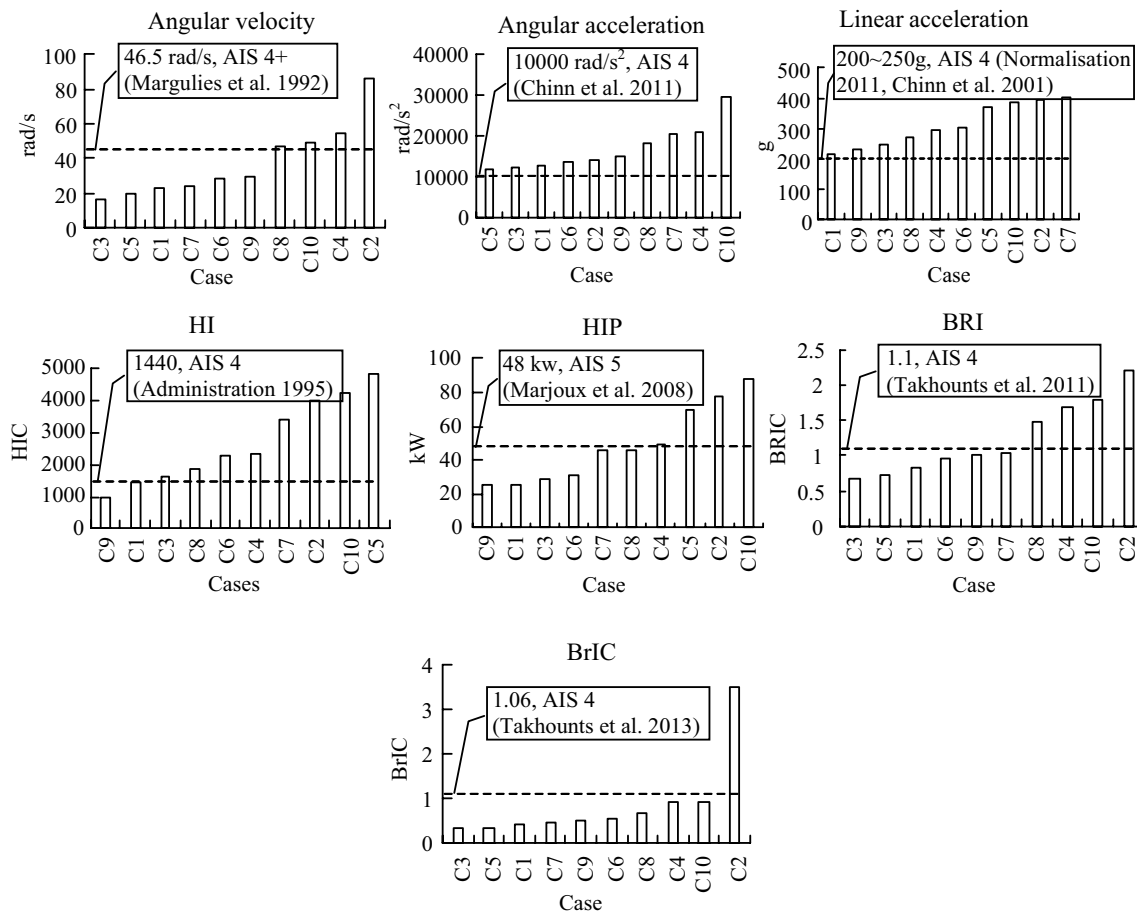
Fig. 4 The prediction result of head injury criteria based on head kinematics

3.2 Brain injury distribution

Table 3 shows the maximum brain tissue criteria value in the ten FE simulations for cases C1–C10. The impact location of the brain and the maximum value location of the VM stress, shear stress and MPS were designated by R and L in each case, where R means the right brain and L means the left brain. The fringe range of the injury criteria value is adjusted in each column based on the threshold in Table 2, the pressure − 234 to 234 kPa, VM stress 0–38 kPa, shear stress 0–11 kPa, and MPS 0–0.9. There is an obvious coup pressure observed on the brain contact side and a contrecoup pressure observed on the opposite side.

For the stress-based criteria, the VM and shear stresses were proportionate to each other in a similar fashion as the principle and shear strains. The locations of the maximum VM and shear stress were quite similar. In particular,

for cases C1, C2, C4, C5, C8, C9 and C10, the maximum stresses were located at the anterior cerebrum adjacent to the cerebral flax (Table 4). In detail, the location of the maximum values of VM stress, shear stress, and MPS were on the cerebrum white matter or gray matter (except for MPS in cases C1 and C6). For the pressure, most of the coup pressure occurred at the cerebrum, while most of the contrecoup pressure occurred at the cerebellum and brain stem.

3.3 Analysis of injury criteria based on head kinematics

The head injury criteria values are compared to the AIS 4+ thresholds of the candidate criteria suggested by the literature (see Fig. 4). For each criterion, the cases have been reordered according to the magnitude of the calculated injury criterion values. The number of well predicted cases for AIS
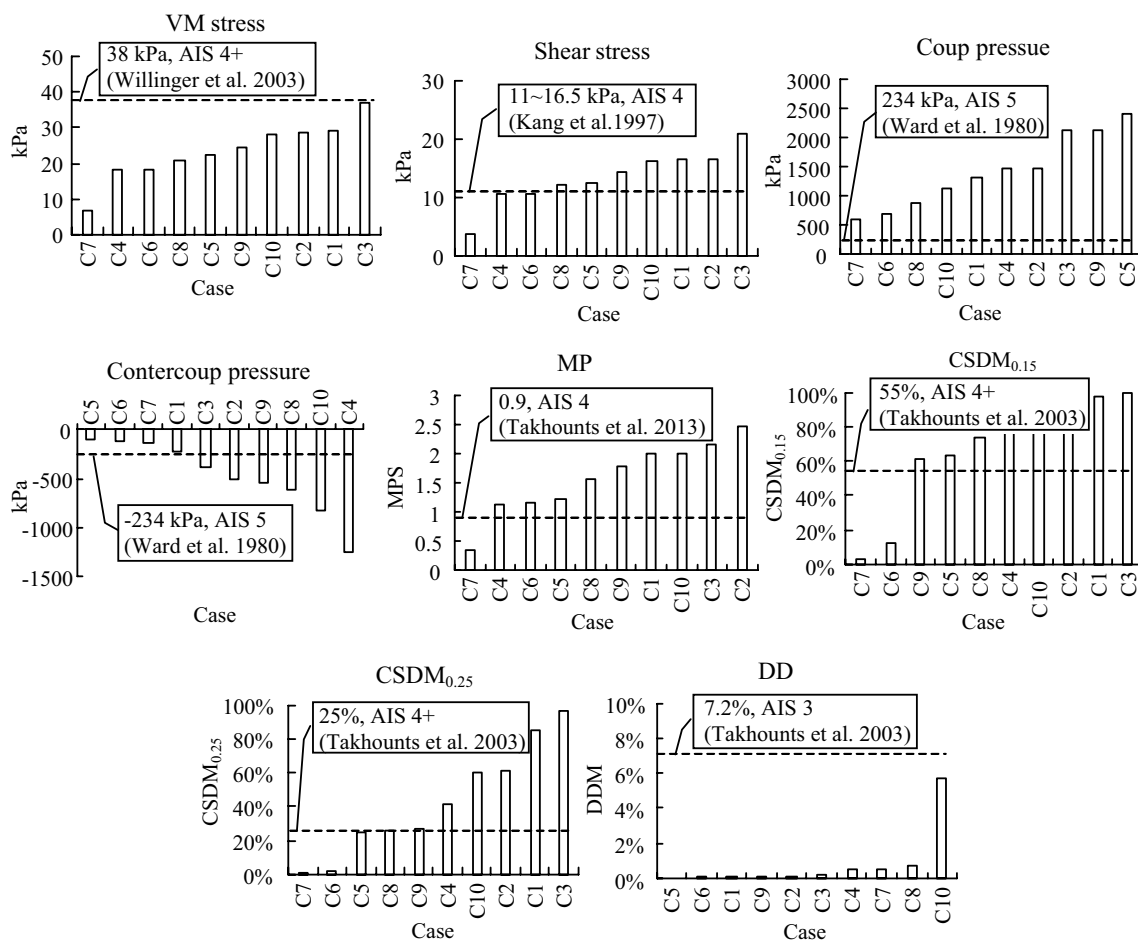
Fig. 5 The prediction result of head injury criteria based on brain tissue response

Fig. 6 Comparison of the capability of various criteria to predict severe head injuries
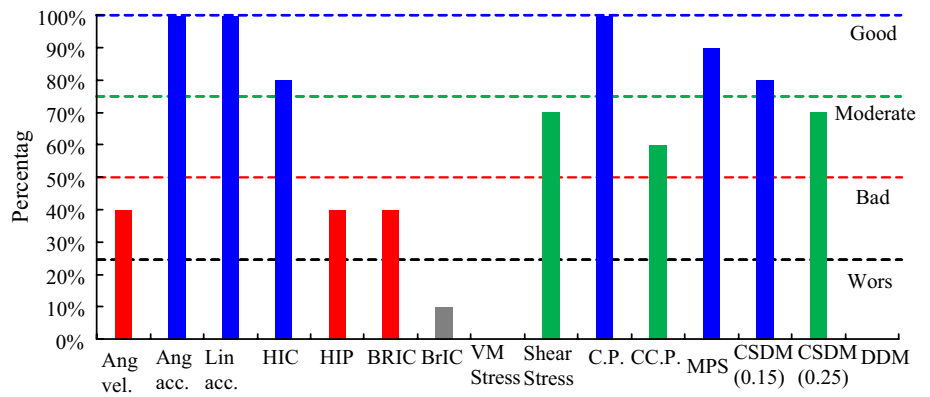
4+ injury (out of the 10 reconstructed cases (in order by angular velocity, angular acceleration, and linear acceleration, HIC, HIP, BRIC, and BrIC) were 4, 10, 10, 8, 4, 4, and 1, respectively. In summary, the predictability of the injury threshold being exceeded by the peak head angular acceleration, linear acceleration, and HIC were superior to those of angular velocity, HIP, BRIC and BrIC. The BrIC shows very limited prediction capability for head sever injury risk. A detailed summary of the simulated injury criteria values is listed in "Appendix" Table 7.

3.4 Analysis of injury criteria based on brain tissue response

Figure 5 shows the head tissue injury criteria values compared to the AIS 4+ thresholds of the candidate criteria as suggested by the literature. The number of well predicted cases by the VM stress, shear stress, coup pressure, contrecoup pressure, MPS, $CSDM_{0.15}$, $CSDM_{0.25}$ and DDM criteria was 0, 7, 10, 6, 9, 8, 7, and 0, respectively. The VM stress and DDM showed very poor prediction capability for head tissue severe injury risk.

Since the estimated head injury criteria were determined for the same set of accidents, the effectiveness of each injury criterion could be compared in terms of its capability of predicting the presence of a severe head injury. Figure 6 shows a synthesis of the prediction capability of each criterion in terms of the brain injuries at AIS 4+. Four assessment levels (good, moderate, poor, and worse) were employed to evaluate the correlation between the criteria and the presence of AIS 4+ head injuries. The results indicated that the angular acceleration, linear acceleration, HIC, coup pressure and MPS showed a good prediction of the severe head injuries as 75–100% of the cases were correctly predicted. The shear stress, contrecoup pressure, and $CSDM_{0.25}$ show a moderate prediction of the severe head injuries as 50–75% of the cases were correctly predicted. The angular velocity, HIP and BRIC showed a poor prediction of the severe head injuries as only 25–50% of the cases were correctly predicted. The BrIC, VM stress and DDM even poorer correlation with severe head injuries as under 25% of the cases were correctly predicted.

Table 5 The prediction capability of good and moderate criteria to the specific injuries

Criteria	SF (Predicted No./cases with SF)	SDH (Predicted No./cases with SDH)	SAH (Predicted No./cases with SAH)
Angular acceleration	6/6	5/5	5/5
Linear acceleration	6/6	5/5	5/5
HIC	6/6	5/5	5/5
Angular velocity	2/6	2/5	1/5
HIP	1/6	2/5	1/5
BRIC	2/6	2/5	1/5
BrIC	0/6	1/5	1/5

4 Discussion

4.1 Influence of video information on the accident reconstruction

In this paper, the video records of the vehicles to VRUs collisions were used to verify the reconstructed VRUs' kinematics during/after vehicle collisions in the simulations. Using these records could improve the reconstruction accuracy compared to reconstructions based on the traditional accident information (trace and final position, et al. without the video records). The main disadvantage of the traditional accident reconstruction was that we could not compare the VRUs' kinematics as well as the body region landing posture, and order of contact during ground impact (Yao et al. 2008; Peng et al. 2012; Bourdet et al. 2014). However, the kinematics of the VRUs show a very important influence on the head injuries (Kendall et al. 2006; Ksimms and Pwood 2006; Shi et al. 2018, 2019). Shi et al. (2018) indicated that different pedestrian landing angles between pedestrians and the ground would causes different head injury risks; and Han et al. (2019b) illustrated that the VRU-to-ground contact sequence has an important influence on head injury severity. The video-based in-depth accident reconstruction could be used to verify the VRU kinematics and ensure the reliability, which is an important basis for analyzing the effectiveness of severe head injury threshold on head-to-ground collision injury prediction.

4.2 Injury criteria based on head kinematics

Seven kinematics-based injury criteria were evaluated using 10 in-depth reconstructed VRU accident cases. The capability of these criteria to predict severe head injury during ground impacts were evaluated by assessing the number of correctly classified injury outcomes in the real accidents (Fig. 4). The linear and angular acceleration correctly predicted the largest number of severe head injuries (skull fracture, SDH, SAH, et al.). The main injury mechanism for a skull fracture resulting from blunt loading is the linear acceleration. While the dominant injury mechanism for SDH and SAH are the transfer of rotational energy at a limited time window to the head (Gennarelli and Thibault 1982; Gennarelli 1983; King et al. 2003).

The capability of the injury criteria to predict the specific injury types was found to have obvious differences (Table 5). For skull fractures, six of all cases recorded with SF have been well predicted by using linear acceleration and HIC.

As the earliest widely analyzed kinematic parameter, the linear acceleration had been found to correlate with the skull fracture (Lissner et al. 1960; Gadd 1966). Likewise, the HIC has been proven as a good predictor of skull fracture (Hertz 1993; Marjoux et al. 2008). For the angular acceleration, Marjoux et al. (2008) indicated that angular acceleration was un-comparable to the linear acceleration for violent cases, while the prediction capability of angular acceleration for the severe injury cases was slightly better than using HIC (Fig. 6). The reason for this inconsistency could be the threshold of 10,000 rad/s^2 used in the current study was a conservative value for AIS 4+ head injuries (Chinn et al. 2001).

The other criteria (angular velocity, HIP, BRIC, and BrIC) were found incapable of predicting severe head injuries. The reason for the poor predictive capability of the maximum angular velocity change was the head rebound motion not being obvious during head contact to the ground (rigid body) as compared to contacts with the vehicle bodies. The process of the head skull fracture absorbing the impact energy could reduce the head rebound motion during ground impacts. The above analysis could explain the BRIC (Takhounts et al. 2011) that considered both angular velocity and acceleration showed better predictive capability than the BrIC (Takhounts et al. 2013) which only considers the peak angular velocities around the three orthogonal axes. Moreover, Takhounts et al. (2011, 2013) proposed these two criteria lack widely accepted verification of applying the human injury data. Regarding the poor prediction of the head impact power (HIP), Newman and Shewchenko (2000) considered not only head linear accelerations but also angular accelerations effects on the head concussion injury. In their study, a HIP value representing a 50% risk of an AIS 3 injury was 12.8 kW. Then, Marjoux et al. (2008) proposed a level of HIP at 48 kW to predict a 50% probability of AIS 5 head injuries. However, in this current study, since the injury of the victims was recorded as AIS 4+, using a HIP value of 48 kW could underestimate the prediction capability of the severe head injury. According to the poor prediction capability of BRIC, HIP and BrIC, and the above analysis, it could be concluded that the head injuries due to ground impact were not likely caused by head rotation but instead resulted from the direct contact to the ground.

4.3 Injury criteria based on brain tissue response

The brain tissue severe injury thresholds were derived based on different human head finite element models.

In particular, the severe injury thresholds for VM stress and maximum shear stress were derived using the ULP (University Louis Pasteur) head FE model (Kang et al. 1997; Willinger and Baumgartner 2003); the severe injury threshold for intracranial pressure was derived using an original FE brain model (Ward et al. 1980). Also, the severe injury thresholds for the strain-based criteria (MPS and CSDM) and dilatational damage measure (DDM) were developed using the SIMon model by scaling the animal's kinematics to humans (Takhounts et al. 2003, 2013). The brain tissue criteria evaluated in this study showed various correlations with the severe head injury, which could be explained by the understanding that brain tissue criteria are sensitive to the choice of brain material properties (Kleiven 2007), that is, the prediction capability of these criteria would be different if difference human head FE models are used.

The THUMS head FE model (Ver. 4.0.2), developed with high precision anatomical features by updating previous head FE model, using improved developments skills, and having more experience (Ward et al. 1980; Kang et al. 1997; Willinger and Baumgartner 2003), could obtain the internal organ responses under various types of loadings. For the shear stress, the threshold was developed using the ULP model (Kang et al. 1997); the short-term (G_0) and long-term (G_1) shear modulus were developed at the time of the development of 49 kPa and 16.7 kPa in the model, respectively. Note that the two shear constants were much stiffer than the materials properties determined by testing experiments on isolated tissue samples (Arbogast et al. 1995; Medige 1997; Darvish and Crandall 2001).The main reason for using the higher shear modulus was to increase the numerical stability. However, the brain material properties of THUMS model used herein were for $G_0 = 6$ kPa and for $G_1 = 1.2$ kPa. These were very close to the reported shear properties of brain tissue in the references (Arbogast et al. 1995; Medige 1997; Darvish and Crandall 2001). That is the reason that the THUMS head FE model should induce a relatively lower stress than the ULP model.

The strain-based brain tissue injury criteria MPS and CSDM could be regarded as the criteria for strain induced axonal injuries (Bandak and Eppinger 1994; Takhounts et al. 2013). The threshold proposed by the SIMon model was used in this current study; however, in the SIMon model, the skull was assumed to be rigid, and the shear moduli were chosen to be $G_0 = 10.3$ kPa and $G_1 = 5$ kPa. These two shear moduli were a little bit stiffer than the average published values determined from the experimental test studies (Arbogast et al. 1995; Medige 1997; Darvish and Crandall

2001), where the average values of G_0 and G_1 are approximately 8 kPa and 3 kPa, respectively. That's the reason that there were nine cases with MPS values exceeding 1.0 and four cases up at 2.0. The good performance of MPS for predicting severe brain injury could be a supplement to the lack of real accident validation data for Takhounts and colleagues' studies (Takhounts et al. 2003). The $CSDM_{0.15}$ showed a slightly better predictive of severe brain injury than $CSDM_{0.25}$, which is consistent with previous studies that showed that a strain level 0.15 provided the best correlation with injuries after undertaking scaled animal test simulations (Takhounts et al. 2003).

For the DDM, none of the simulated cases provided DDM measures that indicated a severe head injury. This result was consistent with the study (Takhounts et al. 2008) that DDM was close to zero for 24 simulated football players impacts. One reason is that the simulated cavitation response should use the "tie-break" contact algorithm (Bandak and Eppinger 1994) that was not used in the THUMS model. Moreover, it is still not clear from the entire research literature whether cavitation occurs or if it caused any injuries. Therefore, the DDM threshold of 7.2% is not suitable for the THUMS head model (Ver. 4.0.2) for predicting the severe brain injuries.

4.4 Limitation

The main limitation for the current study is that there is a limited number of reconstructed accident cases and that there is no case-independent study of pedestrians and two-wheelers. In addition, this study focused on head-to-ground impacts. It is undeniable that intracranial behavior of the brain during head-to-ground collisions may be affected by any preceding kinematics. However, the cumulative effect is not considered for any injury criteria. This could be explained because the effects from the preceding head kinematics were determined to be negligible compared to the violent head-to-ground impact. Moreover, most of the victims were elderly, and half of them suffered the SDH injury. SDH is an injury caused by rupture of the blood vessels in the epidermis of the brain. The importance of SDH for elderly is emphasized by previous studies and that it shows a high mortality rate (Mallory et al. 2011; Mallory 2014). However, there is no venous vessels modeling in THUMS head model and the brain-skull interface was connected with a shared node. As a result, the prediction of SDH cannot be achieved. Therefore, it is necessary to further develop the THUMS intracranial model to explore the mechanism of SDH in the elderly and to derive an SDH injury tolerance for the elderly. In addition, the THUMS model represents a

50th percentile adult. The effects of ages of the victims on the head injury tolerance, which is caused by the differences in brain material properties between adults and the elderly, were not analyzed in the current study. Moreover, the material properties of the THUMS brain model were defined as being linear viscoelastic constitutive properties, which do not simulate the anisotropic nature of the brain tissue. When the brain tissue responded with a small strain, the tissue performed with a soft response, but also demonstrated hardening if the deformation increased (Takhounts et al. 2003). Wang et al. (2018) investigated the effect of different brain constitutive models on brain responses and indicated that using a hyperviscoelastic constitutive property would be a good representation of the nonlinear stress–strain relationship of the brain tissue. Therefore, the result of the current analysis only applied to the THUMS (Ver. 4.0.2) model, and the results demonstrate that the prediction capability of these criteria needs to be investigated more in the further using different head FE models.

Compliance with ethical standards

Conflict of interest The authors declared that they have no conflicts of interest to this work.

Appendix

See Figs. 7, 8 and Tables 6, 7.
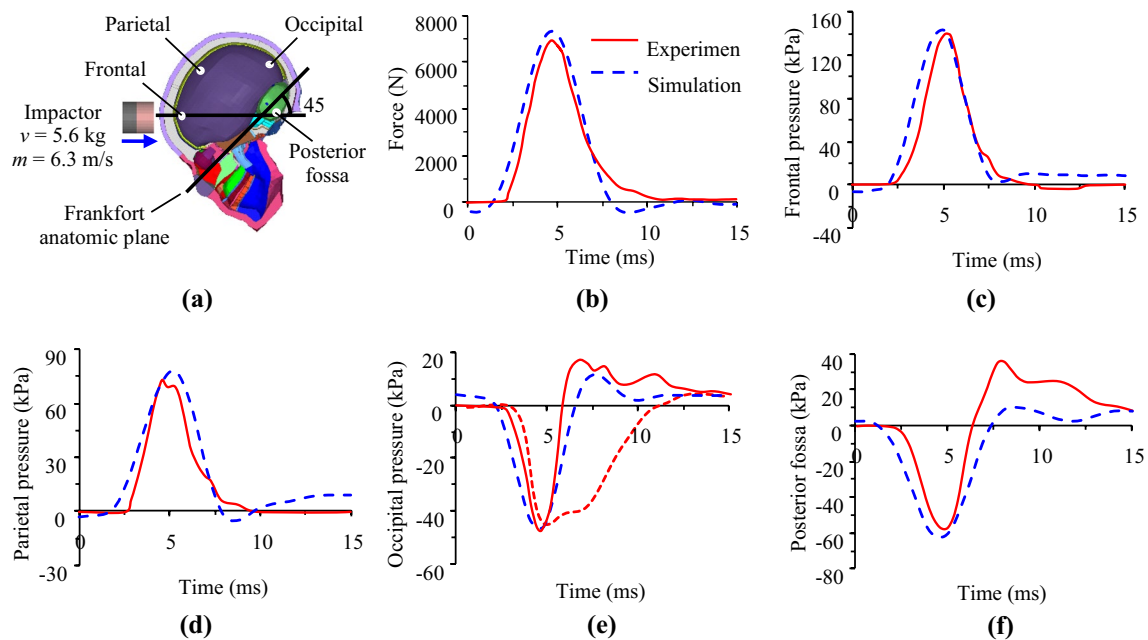
Fig. 7 **a** Frontal impact experiments by Nahum et al. (1977). The comparison between experiment and simulation results: **b** contact force, **c** frontal pressure, **d** parietal pressures, **e** occipital pressure, **f** posterior fossa pressure

Case ID: C1

Case ID: C3

Case ID: C4

Case ID: C5

Case ID: C6-C7
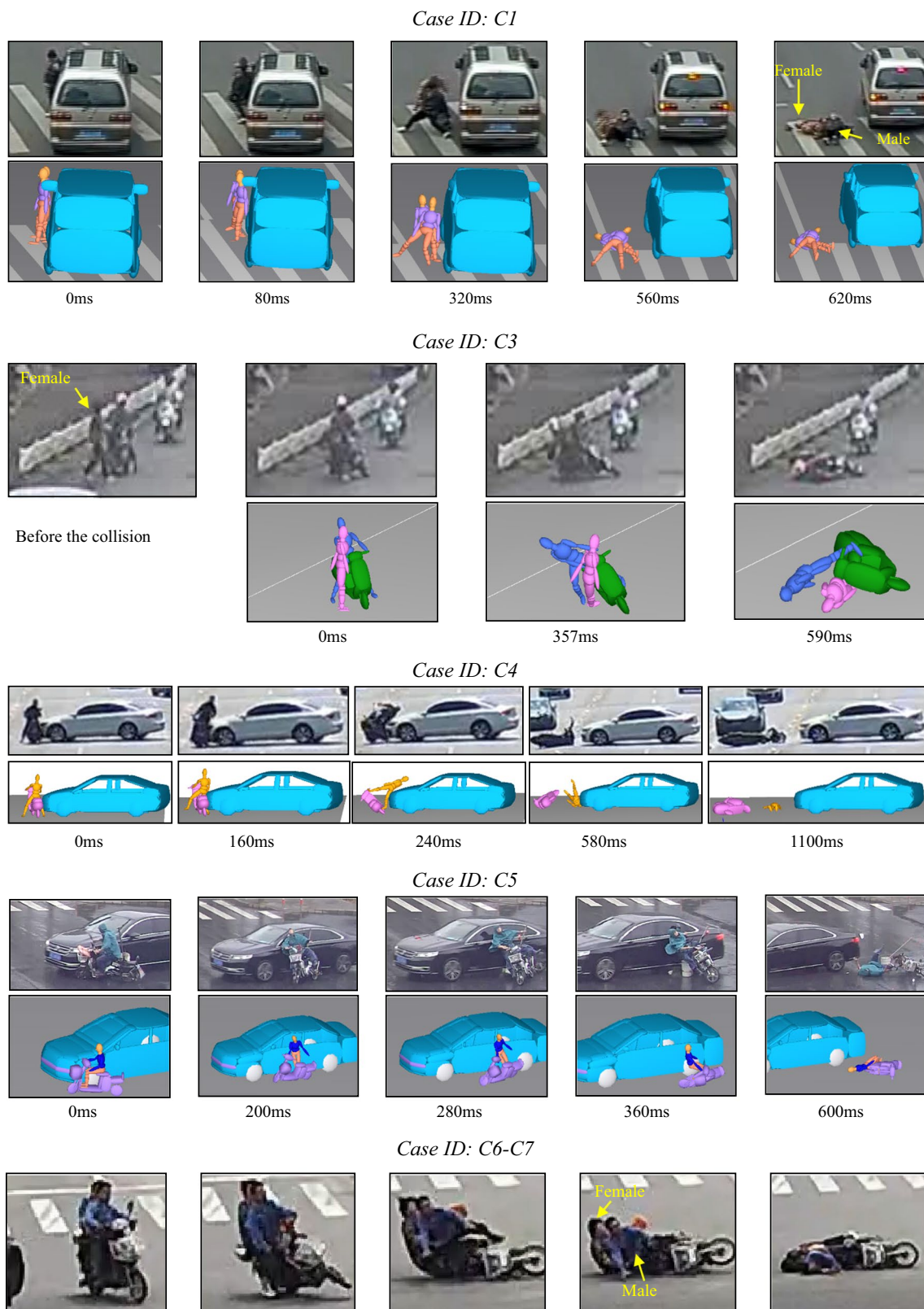
Fig. 8 Comparison of reconstructed kinematics with video screenshots. (In fact, these video screenshots do not really show the video quality. The VRUs body in the screenshots is blurred, but the body can be clearly judged in the video.)

0ms　　　200ms　　　440ms　　　520ms　　　640ms

Case ID: C8

0ms　　　96ms

Case ID: C9

0ms　　　110ms　　　210ms　　　360ms　　　630ms

Case ID: C10

0ms　　　490ms　　　530ms　　　740ms
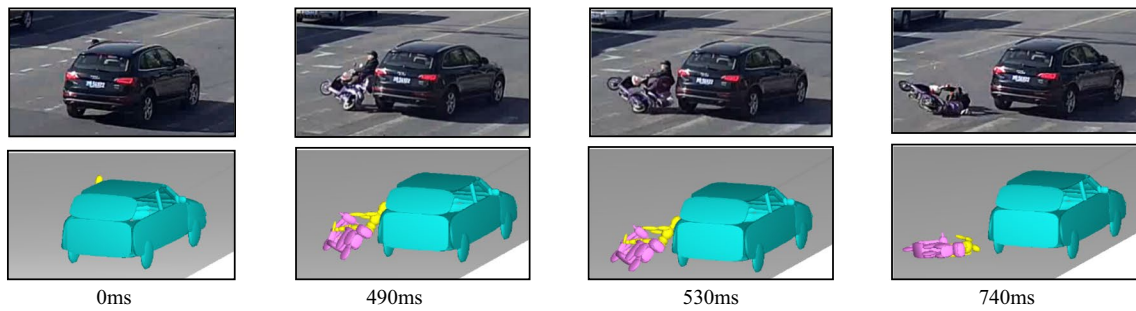
Fig. 8 (continued)

Table 6 Summary of head velocities at the time just before the head-to-ground impact

Case ID	Time to ground impact (ms)	Head linear velocity (m/s)			Head angular velocity (rad/s)		
		v_x	v_y	v_z	ω_x	ω_x	ω_z
C1	683	0.55	−1.41	−4.26	0.01	1.01	−1.14
C2	398	1.33	−3.84	−5.52	−6.45	−1.33	−0.79
C3	687	−0.90	−0.75	−5.15	1.86	−0.55	1.11
C4	572	−3.56	−2.33	−2.96	−2.33	−2.47	1.89
C5	804	0.86	−2.61	−7.07	10.90	0.76	1.61
C6	703	−0.75	−4.61	−4.63	11.47	−15.07	7.24
C7	718	−1.11	−4.44	−5.14	9.53	−7.64	1.97
C8	608	−3.81	−0.48	−2.95	−1.99	−4.57	2.73
C9	670	−1.60	1.77	−3.60	−26.60	0.45	9.02
C10	784	2.25	−2.41	−6.51	37.37	−9.79	5.17

Table 7 Summary of simulated injury criteria values during ground impact

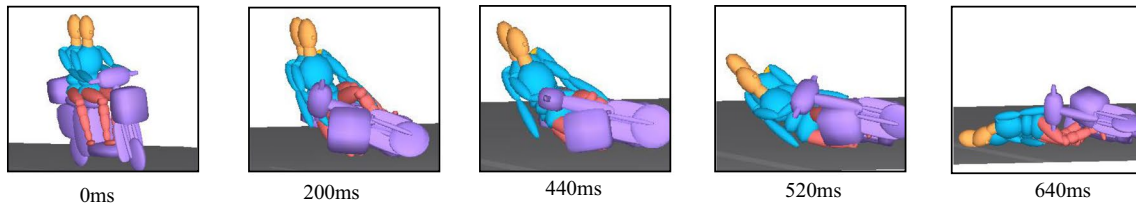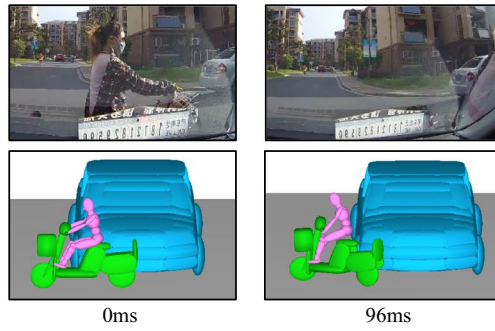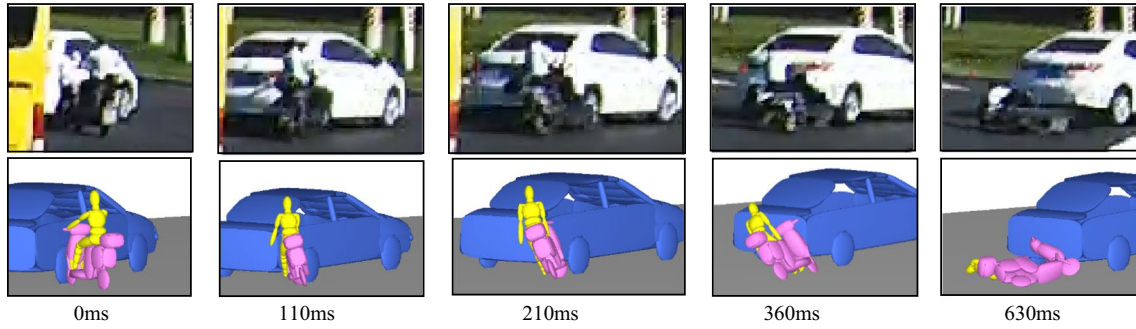| Case ID	Head kinematics-based criteria								Tissue injury criteria							
	Ang.vel. (rad/s)	Ang.acc. (rad/s²)	Lin.acc. (g)	HIC	HIP (kw)	GAMBIT	BRIC	BrIC	VM stress (kPa)	Shear stress (kPa)	C.P. (kPa)	CC.P. (kPa)	MPS	CSDM$_{0.15}$ (%)	CSDM$_{0.25}$ (%)	DDM (%)
C1	23.1	12693	216	1423	26	0.95	0.82	0.41	29.0	16.5	1313	−224	2.00	97.5	84.7	0.02
C2	85.7	14052	394	3998	78	1.80	2.20	3.50	28.8	16.5	1480	−512	2.46	96.0	61.4	0.12
C3	16.4	12095	248	1611	28	1.05	0.66	0.31	36.8	21.0	2107	−390	2.15	99.4	96.0	0.19
C4	54.3	20600	295	2353	49	1.24	1.69	0.91	18.1	10.5	1459	−1256	1.13	85.1	41.2	0.50
C5	20.4	11702	370	4808	70	1.51	0.73	0.31	22.1	12.4	2402	−108	1.22	63.3	24.3	0.00
C6	28.7	13691	302	2286	31	1.27	0.96	0.53	18.4	10.6	682	−118	1.14	12.6	1.9	0.01
C7	24.3	20370	404	3403	45	1.73	1.04	0.45	6.7	3.9	605	−141	0.34	3.4	0.0	0.53
C8	47.4	17810	270	1872	46	1.22	1.47	0.67	20.9	12.0	862	−620	1.56	73.4	26.3	0.70
C9	29.4	15000	230	966	26	1.04	1.01	0.48	24.6	14.2	2125	−547	1.76	61.2	27.2	0.05
C10	48.7	29500	388	4238	89	1.83	1.79	0.91	28.2	16.2	1123	−833	2.00	90.6	60.3	5.70

References

Adams JH, Graham D, Murray LS, Scott G (1982) Diffuse axonal injury due to nonmissile head injury in humans: an analysis of 45 cases. Ann Neurol 12(6):557–563

Anderson RW, Brown C, Blumbergs P, Scott G, Finney J, Jones N, Mclean A (1999) Mechanisms of axonal injury: an experimental and numerical study of a sheep model of head impact. In: Proceedings of the proceedings, international conference on the biomechanics of impact IRCOBI, Sitges, Spain, pp 107–120

Arbogast KB, Meaney DF, Thibault LE (1995) Biomechanical characterization of the constitutive relationship for the brainstem. SAE Technical Paper

Ashton SJ, Mackay GM (1983) Benefits from changes in vehicle exterior design—field accident and experimental work in Europe. In: SAE international

Badea-Romero A, Lenard J (2013) Source of head injury for pedestrians and pedal cyclists: striking vehicle or road? Accid Anal Prev 50:1140–1150

Bain AC, Meaney DF (2000) Tissue-level thresholds for axonal damage in an experimental model of central nervous system white matter injury. J Biomech Eng 122(6):615–622

Bandak FA, Eppinger RH (1994) A three-dimensional finite element analysis of the human brain under combined rotational and translational accelerations. SAE transactions, 1708-1726

Bourdet N, Deck C, Serre T, Perrin C, Llari M, Willinger R (2014) In-depth real-world bicycle accident reconstructions. Int J Crashworthiness 19(3):222–232

Cheng H, Obergefell L, Rizer A (2002) The development of the gebod program. In: Proceedings of the biomedical engineering conference

Chinn B, Canaple B, Derler S, Doyle D, Otte D, Schuller E, Willinger R (2001) Cost 327 motorcycle safety helmets. European Commission, Directorate General for Energy and Transport

Committee EEV-S (1998) Improved test methods to evaluate pedestrian protection afforded by passenger cars. EEVC Working Group 17 Report

Darvish K, Crandall J (2001) Nonlinear viscoelastic effects in oscillatory shear deformation of brain tissue. Med Eng Phys 23(9):633–645

Davidsson J, Angeria M, Risling M (2009) Injury threshold for sagittal plane rotational induced diffuse axonal injuries. In: Proceedings of the proceedings of the international research conference on the biomechanics of impact (IRCOBI), pp 43–56

Denny-Brown D, Russell WR (1941) Experimental cerebral concussion. Brain 64(2–3):93–164

Feng Y, Abney TM, Okamoto RJ, Pless RB, Genin GM, Bayly PV (2010) Relative brain displacement and deformation during constrained mild frontal head impact. J R Soc Interface 7(53):1677–1688

Gabler LF, Crandall JR, Panzer MB (2016) Assessment of kinematic brain injury metrics for predicting strain responses in diverse automotive impact conditions. J Ann Biomed Eng 44(12):3705–3718

Gadd CW (1966) Use of a weighted-impulse criterion for estimating injury hazard. SAE Technical Paper

Gennarelli TA (1983) Head injury in man and experimental animals: clinical aspects. Acta Neurochir 32(32):1–13

Gennarelli TA, Thibault LE (1982) Biomechanics of acute subdural hematoma. J Trauma 22(8):680

Gennarelli TA, Abel JM, Adams H, Graham DJST (1979) Differential tolerance of frontal and temporal lobes to contusion induced by angular acceleration. SAE Trans 88:3503–3514

Gennarelli TA, Thibault LE, Adams JH, Graham DI, Thompson CJ, Marcincin RP (1982) Diffuse axonal injury and traumatic coma in the primate. Ann Neurol 12(6):564–574

Giordano C, Kleiven S (2014) Evaluation of axonal strain as a predictor for mild traumatic brain injuries using finite element modeling. Stapp Car Crash J 58(58):29

Glasson E, Maistre V, Laurent C (2001) Car front end module structure development regarding pedestrian protection and other mechanical constraints. In: SAE international

Han X-Y, Jin X-L, Zhang X-Y, Miao X (2012) Vehicle movement information reconstruction based on video images and dlt theory. Automot Eng 34:1145–1149

Han Y, Li Q, Qian Y, Zhou D, Svensson M (2018) Comparison of the landing kinematics of pedestrians and cyclists during ground impact determined from vehicle collision video records. Int J Veh Saf 10(3–4):212–234

Han Y, He W, Shi L, Wu H, Pan D, Huang H (2019a) Helmet protective performance via reconstruction of electric two-wheeler rider's head-to-ground impact accidents. Int J Crashworthiness 1–11 (in press)

Han Y, Li Q, Wang F, Wang B, Mizuno K, Zhou Q (2019b) Analysis of pedestrian kinematics and ground impact in traffic accidents using video records. Int J Crashworthiness 24(2):211–220

Hardy WN, Foster CD, Mason MJ, Yang KH, King AI, Tashman S (2001) Investigation of head injury mechanisms using neutral density technology and high-speed biplanar X-ray. SAE Technical Paper, pp 337–368

Hardy WN, Mason MJ, Foster CD, Shah CS, Kopacz JM, Yang KH, King AI, Bishop J, Bey M, Anderst W (2007) A study of the response of the human cadaver head to impact. Stapp Car Crash J 51:17

Hertz E (1993) A note on the head injury criterion (hic) as a predictor of the risk of skull fracture. In: Proceedings of the proceedings: association for the advancement of automotive medicine annual conference, pp 303–312

Huang Y, Zhou Q, Koelper C, Li Q, Nie B (2020) Are riders of electric two-wheelers safer than bicyclists in collisions with motor vehicles? Accid Anal Prev 134:105336

Iwamoto M, Kisanuki Y, Watanabe I, Furusu K, Miki K, Hasegawa J (2002) Development of a finite element model of the total human model for safety (thums) and application to injury reconstruction. In: Proceedings of the 2002 international research council on biomechanics of injury, Munich, Germany, pp 31–42

Kang H-S, Willinger R, Diaw BM, Chinn B (1997) Validation of a 3D anatomic human head model and replication of head impact in motorcycle accident by finite element modeling. In: SAE transactions, pp 3849–3858

Kendall R, Meissner M, Crandall J (2006) The causes of head injury in vehicle-pedestrian impacts: comparing the relative danger of vehicle and road surface. In: SAE Technical Paper 1

Kimpara H, Iwamoto M (2012) Mild traumatic brain injury predictors based on angular accelerations during impacts. Ann Biomed Eng 40(1):114–126

King AI, Yang KH, Zhang L, Hardy W, Viano DC (2003) Is head injury caused by linear or angular acceleration. In: Proceedings of the IRCOBI conference

Kleiven S (2007) Predictors for traumatic brain injuries evaluated through accident reconstructions. SAE Technical Paper

Ksimms C, Pwood D (2006) Effects of pre-impact pedestrian position and motion on kinematics and injuries from vehicle and ground contact. Int J Crashworthiness 11(4):345–355

Li G, Yang J, Simms C (2017) Safer passenger car front shapes for pedestrians: a computational approach to reduce overall pedestrian injury risk in realistic impact scenarios. Accid Anal Prev 100:97–110

Lissner H, Lebow M, Evans F (1960) Experimental studies on the relation between acceleration and intracranial pressure changes in man. Surgery, gynecology & obstetrics 111:329

Maki T, Kajzer J (2000) The behavior of bicyclists in frontal and rear crash accidents with cars. JSAE Rev 22(3):357–363

Mallory AE (2014) Measurement of meningeal motion using b-mode ultrasound as a step toward understanding the mechanism of subdural hematoma. The Ohio State University, Columbus

Mallory A, Herriott R, Rhule H (2011) Subdural hematoma and aging: crash characteristics and associated injuries. In: Proceedings of the 22nd international technical conference on the enhanced safety of vehicles (ESV). Washington, DC: Paper

Margulies SS, Thibault LE (1992) A proposed tolerance criterion for diffuse axonal injury in man. J Biomech 25(8):917–923

Marjoux D, Baumgartner D, Deck C, Willinger R (2008) Head injury prediction capability of the hic, hip, simon and ulp criteria. Accid Anal Prev 40(3):1135–1148

Martinez L, Guerra LJ, Ferichola G, Garcia A, Yang J (2007) Stiffness corridors of the european fleet for pedestrian simulations. In: Proceedings of the 20th international technical conference on the enhanced safety of vehicles (ESV) National Highway Traffic Safety Administration

Mclundie W (2007) Investigation of two-wheeled road traffic accidents using explicit FE techniques, Ph.D thesis, Cranfield university

Medige J (1997) Shear properties of human brain tissue. J Biomech Eng 119:423

Mizuno K, Kajzer J (2000) Head injuries in vehicle-pedestrian impact. SAE International

Nahum AM, Smith R, Ward CC (1977) Intracranial pressure dynamics during head impact. SAE Technical Paper, pp 337–366

Newman JA (1986) A generalized acceleration model for brain injury threshold (gambit). In: Proceedings of the proceedings of international IRCOBI conference

Newman JA, Shewchenko N (2000) A proposed new biomechanical head injury assessment function-the maximum power index. SAE Technical Paper

NHTSA (1972) Occupant crash protection–head injury criterion. National Highway Traffic Safety Administration, Washington, DC: (S6. 2 of FMVSS 571.208)

NHTSA (1995) Final economic assessment, FMVSS no. 201, upper interior head protection. National Highway Traffic Safety Administration, Office of Regulatory Analysis, Plans and Policy. Washington DC

Nie B, Zhou Q (2016) Can new passenger cars reduce pedestrian lower extremity injury? A review of geometrical changes of front-end design before and after regulatory efforts. Traffic Injury Prev 17(7):712–719

Normalisation CED (2011) Head and neck impact, burn and noise injury criteria—a guide for cen helmet standards committees. CEN/TR 16148. Comite Europeen de Normalisation

Nusholtz GS, Lux P, Kaiker P, Janicki MA (1984) Head impact response—skull deformation and angular accelerations. SAE Technical Paper

Nusholtz GS, Wylie B, Glascoe LG (1995) Cavitation/boundary effects in a simple head impact model. Aviat Space Environ Med 66(7):661–667

Ommaya AK (1985) Biomechanics of head injuries: experimental aspects. In: Nahum, Melvin (eds) Biomechanics of trauma. Appleton-Century-Crofts, East Norwalk, CT, pp 249–269

Otte D, Pohlemann T (2001) Analysis and load assessment of secondary impact to adult pedestrians after car collisions on roads

Peng Y, Chen Y, Yang J, Otte D, Willinger RM (2012) A study of pedestrian and bicyclist exposure to head injury in passenger car collisions based on accident data and simulations. Saf Sci 50(9):1749–1759

Rosen E, Stigson H, Sander U (2011) Literature review of pedestrian fatality risk as a function of car impact speed. Accid Anal Prev 43(1):25–33

Rowson S, Duma SM, Beckwith JG, Chu JJ, Greenwald RM, Crisco JJ, Brolinson PG, Duhaime A-C, Mcallister TW, Maerlender AC (2012) Rotational head kinematics in football impacts: an injury risk function for concussion. Ann Biomed Eng 40(1):1–13

Sahoo D, Deck C, Willinger R (2016) Brain injury tolerance limit based on computation of axonal strain. Accid Anal Prev 92:53–70

Shi L, Han Y, Huang H, Li Q, Wang B, Mizuno K (2018) Analysis of pedestrian-to-ground impact injury risk in vehicle-to-pedestrian collisions based on rotation angles. J Saf Res 64:37

Shi L, Han Y, Huang H, He W, Wang F, Wang B (2019) Effects of vehicle front-end safety countermeasures on pedestrian head injury risk during ground impact. Proc Inst Mech Eng Part D J Automob Eng 233(14)3588–3599

Shigeta K, Kitagawa Y, Yasuki T (2009) Development of next generation human FE model capable of organ injury prediction. In: Proceedings of the 21st annual enhanced safety of vehicles, pp 15–18

Shin MK, Yi SI, Kwon OT, Park GJ (2008) Structural optimization of the automobile frontal structure for pedestrian protection and the low-speed impact test. Proc Inst Mech Eng Part D J Automob Eng 222(12):2373–2387

Shreiber DI, Bain AC, Meaney DF (1997) In vivo thresholds for mechanical injury to the blood-brain barrier. SAE transactions, pp 3792–3806

Stalnaker R, Alem N, Benson J (1978) Validation studies for head impact injury model US Department of Transportation, National Highway Traffic Safety Administration

Takhounts EG, Eppinger RH, Campbell JQ, Tannous RE, Power ED, Shook LS (2003) On the development of the simon finite element head model. SAE Technical Paper

Takhounts EG, Ridella SA, Hasija V, Tannous RE, Campbell JQ, Malone D, Danelson K, Stitzel J, Rowson S, Duma S (2008) Investigation of traumatic brain injuries using the next generation of simulated injury monitor (SIMon) Finite element head model. SAE Technical Paper

Takhounts EG, Hasija V, Ridella SA, Rowson S, Duma SM (2011) Kinematic rotational brain injury criterion (BRIC). In: Proceedings of the proceedings of the 22nd enhanced safety of vehicles conference. Paper, pp 1–10

Takhounts EG, Craig MJ, Moorhouse K, Mcfadden J, Hasija V (2013) Development of brain injury criteria (BRIC). SAE Technical Paper

Tamura A, Koide T, Yang KH (2014) Effects of ground impact on traumatic brain injury in a fender vault pedestrian crash. Int J Veh Saf 8(1):85–100

Thibault LE, Gennarelli TA, Margulies SS, Marcus J, Eppinger R (1990) The strain dependent pathophysiological consequences of inertial loading on central nervous system tissue. In: Proceedings of the international conference on the biomechanics of impacts, Bron

Trosseille X, Tarriere C, Lavaste F, Guillon F, Domont A (1992) Development of a fem of the human head according to a specific test protocol. SAE Technical Paper

Ueno K, Melvin JW (1995) Finite element model study of head impact based on hybrid III head acceleration: the effects of rotational and translational acceleration. J Biomech Eng 117(3):319–328

Versace J (1971) A review of the severity index. SAE Technical Paper

Wang F, Geng Z, Agrawal S, Han Y, Miller K, Wittek A (2017) Computation of brain deformations due to violent impact: Quantitative analysis of the importance of the choice of boundary conditions and brain tissue constitutive model. In: Computational biomechanics for medicine. Springer, Cham, pp 159–173

Wang F, Han Y, Wang B, Peng Q, Huang X, Miller K, Wittek A (2018) Prediction of brain deformations and risk of traumatic brain injury due to closed-head impact: quantitative analysis of the effects of boundary conditions and brain tissue constitutive model. Biomech Model Mechanobiol 17(4):1165–1185

Wang B, Wang F, Otte D, Han Y, Peng Q (2019) Effects of passenger car front profile and human factors on pedestrian lower extremity injury risk using german in-depth accident data. Int J Crashworthiness 24(2):163–170

Ward C, Chan M, Nahum A (1980) Intracranial pressure—a brain injury criterion. J SAE Transactions, pp 3867–3880

Watanabe R, Miyazaki H, Kitagawa Y, Yasuki T (2011) Research of collision speed dependency of pedestrian head and chest injuries using human FE model (THUMS version 4). In: Proceedings of the 22nd international technical conference on the enhanced safety of vehicles (ESV), WA, pp 11-0043

WHO (2018) Global status report on road safety 2018. World Health Organization, Geneva

Willinger RM, Baumgartner D (2003) Human head tolerance limits to specific injury mechanisms. Int J Crashworthiness 8(6):605–617

Willinger R, Halldin P, Bogerd CP, Deck C, Fahlstedt M (2015) Final report of working group 3: Impact engineering. A cost action TU1101/HOPE collaboration

Yang JK, Lövsund P, Cavallero C, Bonnoit J (2000) A human-body 3d mathematical model for simulation of car-pedestrian impacts. J Crash Prev Inj Control 2(2):131–149

Yao J, Yang J, Otte D (2008) Investigation of head injuries by reconstructions of real-world vehicle-versus-adult-pedestrian accidents. Saf Sci 46(7):1103–1114

Yoganandan N, Li J, Zhang J, Pintar FA, Gennarelli TA (2008) Influence of angular acceleration–deceleration pulse shapes on regional brain strains. J Biomech 41(10):2253–2262

Young JK (1997) Development and validation of a human-body mathematical model for simulation of car-pedestrian collisions. In: IRCOBI conference, pp 14–18

Zhang L, Yang KH, King AI (2004) A proposed injury threshold for mild traumatic brain injury. J Biomech Eng 126(2):226–236

Zou T, Shang S, Simms C (2019) Potential benefits of controlled vehicle braking to reduce pedestrian ground contact injuries. Accid Anal Prev 129:94–107

Publisher's Note Springer Nature remains neutral with regard to jurisdictional claims in published maps and institutional affiliations.